JOURNAL OF INTEGRAL EQUATIONS
AND APPLICATIONS
Volume 22, Number 2, Summer 2010

ELECTRICAL IMPEDANCE TOMOGRAPHY WITH POINT ELECTRODES

FABRICE DELBARY AND RAINER KRESS

Communicated by Kendall Atkinson

Dedicated to Charles Groetsch for
his contributions to integral equations and inverse problems

ABSTRACT. We consider the two-dimensional inverse electrical impedance problem in the case of piecewise constant conductivities with the currents injected at adjacent point electrodes and the resulting voltages measured between the remaining electrodes. Our approach is based on nonlinear integral equations for the unknown shape of an inclusion with conductivity different from the background conductivity. It extends a method that has been suggested by Kress and Rundell [**7**] for the case of a perfectly conducting inclusion. We describe the method in detail and illustrate its feasibility by numerical examples.

1. Introduction. Electrical impedance tomography creates images of the electrical conductivity of a medium by applying currents at a number of electrodes at the boundary and measuring resulting voltages. If $\Omega \subset \mathbf{R}^2$ is a simply connected bounded domain representing the conducting medium, the electric potential u satisfies the potential equation

$$\operatorname{div} \sigma \operatorname{grad} u = 0 \quad \text{in } \Omega$$

with a strictly positive L^∞ function σ representing the isotropic conductivity in Ω. In the classical model, imposing currents on the boundary $\partial\Omega$ is described via a Neumann boundary condition

$$\sigma \frac{\partial u}{\partial \nu} = f \quad \text{on } \partial\Omega$$

This work was supported by the German Ministry of Education and Research in the BMBF-project *Regularization techniques for electrical impedance tomography in medical science and geosiences.*
Received by the editors on September 1, 2009.

DOI:10.1216/JIE-2010-22-2-193

where f is a current density and ν is the outward unit normal to $\partial\Omega$. The measured voltages are represented by the boundary trace $g := u|_{\partial\Omega}$ and the classical inverse impedance tomography problem consists in recovering information on σ from a number of current and voltage pairs (f, g).

In a more realistic model, following [**10**], the electrodes are considered as connected open subsets $\mathcal{E}_p \subset \partial\Omega$ with the imposed currents given by

$$\int_{\mathcal{E}_p} \sigma \frac{\partial u}{\partial \nu}\, ds = I_p, \quad p = 1, \dots, n.$$

The measured voltages at the electrodes and the vanishing currents on the space $\mathcal{N}$ between the electrodes are modeled by the boundary conditions

$$u + z_p \sigma \frac{\partial u}{\partial \nu} = U_p \text{ on } \mathcal{E}_p, \quad p = 1, \dots, n,$$

and

$$\frac{\partial u}{\partial \nu} = 0 \text{ on } \mathcal{N},$$

where z_p denotes a constant contact impedance of the electrode $\mathcal{E}_p$. The inverse impedance tomography problem in the framework of the complete electrode model consists in recovering information on the conductivity σ from a number of pairs of imposed currents $I_1, \dots, I_n$ and measured voltages $U_1, \dots, U_n$.

However, the more complicated form of the boundary condition in the complete electrode model leads to severe difficulties in numerical approximations both via finite element or boundary element methods due to singularities of the solution u at the end points of each of the electrodes. Since on the other hand, the accuracy of reconstructions via impedance tomography suffers from ambiguities for the location both of the boundary itself and the electrodes [**5**], without any loss of accuracy in reconstructions, it might be appropriate to use a simpler model for the current injection, for example, by considering point electrodes as investigated in this paper.

In a number of applications of impedance tomography the conductivity in Ω has the property to be of high contrast. This, for example, is the case for the human thorax where the conductivity within the lungs is much smaller than the conductivity in the neighboring tissues. Also in geophysical explorations the contrast between minerals

and the surrounding soil can be quite large. In such a situation it seems natural to approximate the conductivity by a piecewise constant function. Then inverse impedance tomography simplifies into an inverse transmission problem with the boundaries of the unknown subdomains and their respective constant conductivities as unknowns. This inverse transmission problem may now be treated via boundary integral equation methods. In our investigations on impedance tomography with point electrodes we also will confine ourselves to the case of piecewise constant conductivities.

More precisely, we will study the inverse problem to recover the shape of an inclusion D, supposed to be a simply connected bounded Lipschitz domain with constant conductivity σ_1 in a homogeneous medium Ω with conductivity σ_0. As background medium Ω we consider either a disk or a half plane. The configuration of the disk covers medical imaging of the human thorax via impedance tomography and the case of the half plane models applications in geophysical exploration. We position n point electrodes ℓ_p on the boundary $\partial\Omega$ and denote their location by x_p for $p = 1, \ldots, n$ such that ℓ_p is adjacent to ℓ_{p+1} (with the convention that $x_{n+1} = x_1$). For each adjacent pair of electrodes a current I_p is imposed between the electrodes located at x_p and x_{p+1}, and this is modeled by the Neumann boundary condition

$$\sigma_0 \frac{\partial u}{\partial \nu} = I_p(\delta_{x_p} - \delta_{x_{p+1}}) \quad \text{on } \partial\Omega$$

in terms of the Dirac distribution. The inverse impedance tomography problem we are concerned with is to recover an approximation of the shape of the inclusion D from the measured voltages between the other pairs of electrodes.

For the solution of this inverse problem we propose a variant of a nonlinear integral equation method that originally was suggested by Kress and Rundell [**7**] for the inverse problem to recover the shape of a perfectly conducting medium D from measured Cauchy data on the boundary $\partial\Omega$. This method has also been successfully extended by Eckel and Kress [**1, 2**] to inverse impedance tomography with piecewise constant conductivities both for the case of Cauchy data on $\partial\Omega$ and for the complete electrode model. In the current setting, basically it consists in representing the solution of the transmission problem as a single-layer potential in terms of the Green's function for the

Neumann problem for Ω. Then the transmission condition transform into a well-posed boundary integral equation over ∂D for the density φ of the potential that might be considered as the field equation. The measured potentials at the electrodes for the various current inputs then lead to a second and ill-posed equation in terms of the density φ and the boundary ∂D that we might denote as data equation. Then, roughly speaking, given a current approximation for the boundary ∂D we can solve the well-posed field equation for φ. After this, keeping φ fixed, we linearize the data equation with respect to ∂D to update the boundary approximation via regularization of the linearized equation. This procedure is iterated until some stopping criterium is satisfied. Given a reasonable initial guess, we will provide numerical evidence for practicality of the method.

Although for simplicity we assume that we have only one inclusion, our approach extends to the case of a finite number of disjoint inclusions provided we know the number of components in advance and have reasonable a priori information on their size and location to start the iteration. This information, for example, could be retrieved from so-called qualitative methods such as the factorization method [**3**].

The plan of our presentation is as follows: In Section 2 we present an existence analysis for the direct problem under the assumption of a Lipschitz boundary for D including the numerical solution. Then in Section 3 we proceed with the detailed description of the proposed inverse algorithm. In both sections we concentrate on the case of a disk Ω as background medium and treat the case where Ω is a half plane only in passing. The paper is concluded with some numerical examples in Section 4 illustrating the feasibility of the proposed algorithm.

2. The direct problem. We begin by considering the case of an open disk Ω of radius R centered at the origin and denote its boundary by $\Gamma := \partial\Omega$. Assume that D is a simply connected Lipschitz domain with $\overline{D} \subset \Omega$. Both for Ω and D we will denote the outward normal by ν. The trace of a sufficiently regular function u from outside a domain will be denoted by u_+ and the trace from inside by u_-. The same notations will be used for the normal derivatives $\partial_\nu u_+$ and $\partial_\nu u_-$. In terms of the constant conductivities σ_1 of the inclusion D and σ_0 of the background $\Omega \setminus D$ we define the piecewise constant conductivity σ by

$$\sigma = \begin{cases} \sigma_0 & \text{in } \Omega \setminus \overline{D}, \\ \sigma_1 & \text{in } D. \end{cases}$$

Denote the locations of two electrodes on the boundary Γ by x_+ and x_- and impose a current I between x_+ and x_-. In terms of the fundamental solution to the Laplace equation given by

$$\Phi(x,y) = \frac{1}{2\pi} \ln \frac{1}{|x-y|}, \quad x \neq y,$$

we introduce a harmonic function Λ in $\mathbf{R}^2 \setminus \{x_+, x_-\}$ by setting

$$\Lambda(x, x_+, x_-) := \frac{2I}{\sigma_0} \{\Phi(x, x_+) - \Phi(x, x_-)\}, \quad x \neq x_+, x_-. \tag{2.1}$$

Formally, the forward problem amounts to seeking a solution u_0 to the potential equation

$$\operatorname{div} \sigma \operatorname{grad} u_0 = 0 \quad \text{in } \Omega$$

subject to the boundary condition

$$\sigma_0 \frac{\partial u_0}{\partial \nu} = I(\delta_{x_+} - \delta_{x_-}) \quad \text{on } \Gamma.$$

Since Λ satisfies

$$\sigma_0 \frac{\partial \Lambda}{\partial \nu} = I(\delta_{x_+} - \delta_{x_-}) \quad \text{on } \Gamma$$

in the distributional sense, the above problem can be cast into finding a function $u \in H^1(\Omega)$ such that

$$\operatorname{div} \sigma \operatorname{grad} (u + \Lambda) = 0 \quad \text{in } \Omega \tag{2.2}$$

and

$$\sigma_0 \frac{\partial u}{\partial \nu} = 0 \quad \text{on } \Gamma. \tag{2.3}$$

Here, physically speaking, Λ represents the imposed potential and u stands for the induced potential. Using the fact that Λ is harmonic in Ω, the problem (2.2)–(2.3) can be equivalently written as finding $u \in H^1(\Omega)$ satisfying the Laplace equation

$$\Delta u = 0 \quad \text{in } \Omega \setminus \partial D, \tag{2.4}$$

the homogeneous Neumann boundary condition

$$\frac{\partial u}{\partial \nu} = 0 \quad \text{on } \Gamma \tag{2.5}$$

and the transmission conditions

$$u_+ - u_- = 0 \quad \text{on } \partial D \tag{2.6}$$

and

$$\sigma_0 \frac{\partial u}{\partial \nu}_+ - \sigma_1 \frac{\partial u}{\partial \nu}_- = -(\sigma_0 - \sigma_1) \frac{\partial \Lambda}{\partial \nu} \quad \text{on } \partial D. \tag{2.7}$$

Since (2.4)–(2.7) define the potential u only up to an additive constant, we impose

$$\int_\Gamma u \, ds = 0 \tag{2.8}$$

as an additional normalization condition.

2.1. Existence and uniqueness.

Theorem 2.1 *The direct problem* (2.4)–(2.8) *has at most one solution.*

Proof. Assume that u is the difference of two solutions. Then, in view of (2.4)–(2.7), Green's integral theorem yields $\int_\Omega \sigma |\operatorname{grad} u|^2 \, dx = 0$. Together with (2.6), this implies $u = \text{const}$ in Ω and (2.8) enforces $u = 0$ in Ω. □

To establish the existence of a solution we employ a single-layer potential approach using the Green's function for the Neumann problem in the disk Ω. To this end, noting that $R^2 y/|y|^2 \in \mathbf{R}^2 \setminus \overline{\Omega}$ for all $y \in \Omega$, we define a function Φ_c on $\Omega \times \Omega$ by

$$\Phi_c(x, y) = \frac{1}{2\pi} \ln \left(\frac{R}{|y| \left| x - \frac{R^2 y}{|y|^2} \right|} \right), \quad x, y \in \Omega. \tag{2.9}$$

Since for all $x, y \in \Omega$ we have that

$$\frac{1}{R^2}\,|y|^2\left|x - \frac{R^2 y}{|y|^2}\right|^2 = R^2 - 2\,x\cdot y + \frac{|x|^2|y|^2}{R^2} \neq 0,$$

we observe that Φ_c is symmetric and harmonic in Ω both with respect to x and y. Moreover, it can be verified that

$$\frac{\partial}{\partial\nu(x)}\left\{\Phi(x,y) + \Phi_c(x,y)\right\} = -\frac{1}{2\pi R}, \quad x \in \Gamma,\ y \in \Omega. \tag{2.10}$$

For densities $\varphi \in H^{-1/2}(\partial D)$, we introduce the single-layer potential

$$(S\varphi)(x) := \int_{\partial D} \Phi(x,y)\varphi(y)\,ds(y), \quad x \in \mathbf{R}^2.$$

(As usual, integrals on $H^{-1/2}(\partial D)$ have to be understood in the sense of the duality pairing.) Then, the normal traces of $S\varphi$ on ∂D are given by

$$\frac{\partial}{\partial\nu}\,(S\varphi)_{\pm} = \mp\frac{\varphi}{2} + \frac{1}{2}\,K'\varphi \tag{2.11}$$

where $K' : H^{-1/2}(\partial D) \to H^{-1/2}(\partial D)$ is defined by

$$(K'\varphi)(x) := 2\int_{\partial D} \frac{\partial\Phi(x,y)}{\partial\nu(x)}\,\varphi(y)\,ds(y), \quad x \in \partial D. \tag{2.12}$$

Further we define the potential

$$(S_c\varphi)(x) := \int_{\partial D} \Phi_c(x,y)\varphi(y)\,ds(y), \quad x \in \Omega.$$

Since the kernel Φ_c is regular the normal trace of $S_c\varphi$ on ∂D is simply given by

$$\frac{\partial}{\partial\nu}\,(S_c\varphi) = \frac{1}{2}\,K_c'\varphi \tag{2.13}$$

where $K_c' : H^{-1/2}(\partial D) \to H^{-1/2}(\partial D)$ is defined by

$$(K_c'\varphi)(x) := 2\int_{\partial D} \frac{\partial\Phi_c(x,y)}{\partial\nu(x)}\,\varphi(y)\,ds(y), \quad x \in \partial D. \tag{2.14}$$

As the kernel Φ_c is regular, for all $\varphi \in H^{-1/2}(\partial D)$, we have that$K_c'\varphi \in L^2(\partial D)$ and since the injection $L^2(\partial D) \hookrightarrow H^{-1/2}(\partial D)$ is compact the operator K_c' is compact.

We now try to find a solution to problem (2.4)–(2.8) in the form of the sum of a single layer potential S and a potential S_c. For convenience we set

$$\mu = \frac{\sigma_0 - \sigma_1}{\sigma_0 + \sigma_1}$$

and note that $\mu \in (-1, 1)$ as consequence of $\sigma_0, \sigma_1 > 0$.

Theorem 2.2. *Assume that $\varphi \in H^{-1/2}(\partial D)$ is a solution to boundary integral equation*

$$\varphi - \mu K'\varphi - \mu K_c'\varphi = 2\mu \frac{\partial \Lambda}{\partial \nu}. \tag{2.15}$$

Then

$$\int_{\partial D} \varphi \, ds = 0 \tag{2.16}$$

and

$$u = S\varphi + S_c\varphi \tag{2.17}$$

solves the transmission problem (2.4)–(2.8).

Proof. Clearly, (2.17) defines $u \in H^1(\Omega)$ satisfying (2.4) and (2.6). Via (2.11) and (2.13) the integral equation (2.15) ensures that the transmission condition (2.7) is satisfied. Since $S_c\varphi$ is harmonic in D, in view of (2.13) we have that

$$\int_{\partial D} K_c'\varphi \, ds = 0. \tag{2.18}$$

Similarly, since $S\varphi$ is harmonic in D from the second equation of (2.11) we deduce

$$\int_{\partial D} \varphi \, ds + \int_{\partial D} K'\varphi \, ds = 0 \tag{2.19}$$

and adding both equations we arrive at

$$\int_{\partial D} \varphi \, ds + \int_{\partial D} \{K'\varphi + K_c'\varphi\} \, ds = 0.$$

On the other hand, observing that Λ is harmonic in D from the integral equation (2.15) we obtain

$$\int_{\partial D} \varphi \, ds - \mu \int_{\partial D} \{K'\varphi + K_c'\varphi\} \, ds = 0$$

and together with the previous equation in view of $\mu \neq -1$ this implies (2.16). Now putting (2.10) and (2.16) together, for $x \in \Gamma$ we find

$$\begin{aligned} \frac{\partial u}{\partial \nu}(x) &= \int_{\partial D} \frac{\partial}{\partial \nu(x)} \{\Phi(x,y) + \Phi_c(x,y)\} \, \varphi(y) \, ds(y) \\ &= -\frac{1}{2\pi R} \int_{\partial D} \varphi \, ds = 0, \end{aligned}$$

i.e., the Neumann boundary condition (2.5) is satisfied.

The potential with constant density

$$w(y) := \int_{\Gamma} \{\Phi(x,y) + \Phi_c(x,y)\} \, ds(x), \quad y \in \Omega,$$

is harmonic in Ω and, by symmetry, is constant on the boundary Γ. Hence, by the maximum-minimum principle $w = w_0$ in Ω for some constant w_0. Interchanging the order of integration, this finally implies

$$\int_{\Gamma} u \, ds = \int_{\Gamma} \{S\varphi + S_c\varphi\} ds = \int_{\partial D} w\varphi \, ds = w_0 \int_{\partial D} \varphi \, ds,$$

and as consequence of (2.16) we observe that the normalization condition (2.8) is also satisfied. □

Note that the condition (2.16) is usually imposed in order to insure the boundedness of the single-layer potential at infinity. Here, this condition is automatically satisfied for any solution of the boundary integral equation (2.15). This is quite interesting from a numerical point of view since for the computations of the solution to the forward

problem, the equation (2.15) is directly usable without any modification and the spaces used for the discretization do not have to be adapted.

Now, the loss of compactness for the operator K' for non regular domains involves a proof of existence different than the one for domains of class C^2 where the Riesz-Fredholm theory is sufficient since the operator K' is compact [**6**] and also K'_c is compact as pointed out above. In order to keep a general framework, we will first prove the existence of a solution to the integral equation (2.15) for Lipschitz domains. After this we will briefly describe the analysis for more regular domains. We define

$$H_0^{-1/2}(\partial D) := \left\{ \varphi \in H^{-1/2}(\partial D) : \int_{\partial D} \varphi = 0 \right\}$$

and note that K' maps $H_0^{-1/2}(\partial D)$ into itself as consequence of (2.19).

Theorem 2.3. *The operator $I - \mu K' : H_0^{-1/2}(\partial D) \to H_0^{-1/2}(\partial D)$ has a bounded inverse.*

Proof. We introduce the single-layer operator $S_0 : H^{-1/2}(\partial D) \to H^{1/2}(\partial D)$ by

$$(S_0\varphi)(x) := \int_{\partial D} \Phi(x,y)\varphi(y)\, ds(y), \quad x \in \partial D,$$

and assume that the diameter $\operatorname{diam}(\partial D)$ of ∂D is less than 1. In this case, the operator S_0 is positive and strictly coercive and the so-called energy norm given by

$$||\varphi||_{S_0} := \sqrt{\int_{\partial D} \varphi S_0 \overline{\varphi}\, ds}$$

is equivalent to the $H^{-1/2}(\partial D)$ norm (see [**8**]). In [**11**] it is shown that

$$\max\left\{ \|(I + K')\varphi\|_{S_0}, \|(I - K')\varphi\|_{S_0} \right\} \leq c\|\varphi\|_{S_0}$$

for all $\varphi \in H_0^{-1/2}(\partial D)$ and some constant $0 < c < 2$. Since $\mu \in (-1,1)$ we have that $(1+\mu)/2$ and $(1-\mu)/2$ both are positive. Therefore, writing

$$I + \mu K' = \frac{1+\mu}{2}(I + K') + \frac{1-\mu}{2}(I - K'),$$

we can estimate

$$\|(I+\mu K')\varphi\|_{S_0} \leq \frac{1+\mu}{2} c\|\varphi\|_{S_0} + \frac{1-\mu}{2}\, c\|\varphi\|_{S_0} \leq c\|\varphi\|_{S_0}$$

for all $\varphi \in H_0^{-1/2}(\partial D)$. Consequently, the Neumann series for the operator

$$\frac{1}{2}\,(I-\mu K') = I - \frac{1}{2}\,(I+\mu K')$$

converges and the theorem is proven in the case where diam $(\partial D) < 1$.

Finally, from

$$\frac{\partial}{\partial \nu(x)}\,\Phi(x,y) = \frac{1}{2\pi}\,\frac{\nu(x)\cdot\{y-x\}}{|y-x|^2}$$

it can be seen that K' is invariant with respect to scaling of ∂D, i.e., for the domain D and $\alpha D := \{\alpha x : x \in D\}$ for $\alpha > 0$ the kernels of K' coincide. Therefore, the result of the theorem remains valid also for diam $(\partial D) \geq 1$. □

Corollary 2.4. *The transmission problem* (2.4)–(2.8) *has a unique solution.*

Proof. According to the previous Theorem 2.3, the operator $I-\mu K'$ has a bounded inverse on $H_0^{-1/2}(\partial D)$. Remarking that K_c' as a consequence of (2.18) also maps $H_0^{-1/2}(\partial D)$ into itself, and recalling that it is compact we observe that $I-\mu K'-\mu K_c'$ is a Fredholm operator of index zero. Moreover, according to Theorems 2.1 and 2.2 the operator $I-\mu K'-\mu K_c'$ is injective and therefore bijective. □

As stated before, if the boundary of D is supposed to be of class C^2 then from (2.21) it can be seen that the operator K' has a continuous kernel and consequently $K' : H^{-1/2}(\partial D) \to H^{-1/2}(\partial D)$ is compact. Hence, in this case we immediately have that $I-\mu K'-\mu K_c'$ is a Fredholm operator of index zero without appealing to the techniques of the proof of Theorem 2.3. Furthermore, since in this case $\partial_\nu \Lambda$ is in $C^2(\partial D)$, we also may consider $I-\mu K'-\mu K_c'$ as an operator from the Hölder space $C^{0,\alpha}(\partial D)$ into itself with compact operators K'

and K_c'. Moreover, this consideration allows us to establish stronger regularity results on u. Indeed, in this case $u|_{\overline{D}} \in C^{1,\alpha}(\overline{D})$ and $u|_{\overline{\Omega}\setminus D} \in C^{1,\alpha}(\overline{\Omega}\setminus D)$.

In concluding this subsection we note that in view of the fact that $\Phi+\Phi_c$ corresponds to the Neumann function for the Laplace equation in the disk of radius R our analysis can be extended to arbitrary domains Ω.

2.2. On the numerical solution. For the numerical solution we propose to use the Nyström method as described in [**6**] for boundary value problems for the Laplace equation. For simplicity we assume that D is of class C^2 with a regular parameterization

$$\partial D = \{z(t) : t \in [0,2\pi]\} \tag{2.20}$$

with $|z'(t)| > 0$ for all $t \in [0,2\pi]$ and counter clockwise orientation. We introduce an integral operator $A : H_0^{-1/2}[0,2\pi] \to H_0^{-1/2}[0,2\pi]$ in terms of the kernels

$$L(t,\tau) = \frac{1}{\pi} \frac{\{z(\tau)-z(t)\}\cdot[z'(t)]^\perp}{|z(t)-z(\tau)|^2} \frac{|z'(\tau)|}{|z'(t)|} \tag{2.21}$$

and

$$L_c(t,\tau) = \frac{1}{\pi} \frac{\left\{\frac{R^2 z(\tau)}{|z(\tau)|^2} - z(t)\right\}\cdot[z'(t)]^\perp}{\left|z(t)-\frac{R^2 z(\tau)}{|z(\tau)|^2}\right|^2} \frac{|z'(\tau)|}{|z'(t)|} \tag{2.22}$$

for $t,\tau \in [0,2\pi]$ by

$$(A\psi)(t) := \int_0^{2\pi} \{L(t,\tau)+L_c(t,\tau)\}\,\psi(\tau)\,d\tau, \quad t \in [0,2\pi], \tag{2.23}$$

and the parameterized right-hand side

$$\lambda(t,x_+,x_-) := \frac{I}{\pi\sigma_0}\left[\frac{\{x_+-z(t)\}\cdot[z'(t)]^\perp}{|z(t)-x_+|^2|z'(t)|} - \frac{\{x_--z(t)\}\cdot[z'(t)]^\perp}{|z(t)-x_-|^2|z'(t)|}\right] \tag{2.24}$$

for $t \in [0,2\pi]$ where $[z'(t)]^\perp = (z_2'(t), -z_1'(t))$ for $z(t) = (z_1(t), z_2(t))$. Then the integral equation (2.15) assumes the parameterized form

$$\psi - \mu A\psi = 2\mu\lambda(\cdot,x_+,x_-) \tag{2.25}$$

for $\psi := \varphi \cdot z$. The kernels L and L_c are continuous with the diagonal term of L given by

$$L(t,t) = \frac{1}{2\pi} \frac{z''(t) \cdot [z'(t)]^{\perp}}{|z'(t)|^2}, \quad t \in [0, 2\pi].$$

For analytic boundaries both kernels turn out to be analytic. Now the Nyström method with the composite trapezoidal rule can be applied for (2.25) with exponential convergence for analytic boundaries.

2.3. The half plane case. In the case where Ω is either the upper or lower half plane we are seeking for a function $u \in H^1_{\mathrm{loc}}(\Omega)$ and in the formulation (2.4)–(2.8) of the transmission problem the normalization condition (2.8) has to be replaced by the decay condition

$$u(x) \longrightarrow 0, \quad |x| \to \infty, \tag{2.26}$$

uniformly for all directions in Ω. For each $x = (x_1, x_2) \in \mathbf{R}^2$ we denote by $\overline{x} = (x_1, -x_2)$ its mirror point at the x_1-axis. Then we note that the function

$$\widetilde{u}(x) := \begin{cases} u(x) & x \in \Omega, \\ u(\overline{x}) & x \in \mathbf{R}^2 \setminus \overline{\Omega}, \end{cases}$$

is continuous across $\Gamma = \partial\Omega$ and so is its normal derivative because of the homogeneous Neumann condition (2.5). Hence, $\widetilde{u}$ is harmonic outside some sufficiently large disk. This implies that the condition (2.26) is equivalent to

$$u(x) = O\left(\frac{1}{|x|}\right), \quad \operatorname{grad} u(x) = O\left(\frac{1}{|x|}\right), \quad |x| \to \infty,$$

(see [**6**]). Therefore (2.26) can be seen to ensure the existence of the integral $\int_\Omega \sigma |\operatorname{grad} u|^2 \, dx$ from the proof of the uniqueness Theorem 2.1.

For the existence analysis we replace (2.9) by

$$\Phi_c(x,y) = \Phi(x, \overline{y}). \tag{2.27}$$

Then

$$\frac{\partial}{\partial \nu(x)} \{\Phi(x,y) + \Phi_c(x,y)\} = 0, \quad x \in \Gamma, \ y \in \Omega. \tag{2.28}$$

With this modification the analysis from the case of the disk immediately carries over to the half plane case and, in particular, Theorems 2.2 and 2.3 and Corollary 2.4 remain valid. For the numerical solution the expression (2.22) for the kernel L_c has to be replaced by

$$L_c(t,\tau) = \frac{1}{\pi} \frac{\{\overline{z}(\tau) - z(t)\} \cdot [z'(t)]^{\perp}}{|z(t) - \overline{z}(\tau)|^2} \frac{|z'(\tau)|}{|z'(t)|} \tag{2.29}$$

for $t, \tau \in [0, 2\pi]$.

3. The inverse algorithm. We recall that the inverse problem consists in applying for each adjacent pair of electrodes ℓ_p and ℓ_{p+1} a current I_p and recover an approximation of the shape of the inclusion D from the measured voltages V_{pq} between the other pairs of electrodes ℓ_q and ℓ_{q+1} for $q \notin \{p-1, p, p+1\}$. For the sake of simplicity, we will use the same current I for all $p = 1, \ldots, n$. Furthermore, in this initial investigation of our approach we consider the conductivities as known.

For the evaluation of (2.17) we note that

$$(S_c\varphi)(x) = (S\varphi)(x), \quad x \in \Gamma, \tag{3.1}$$

as consequence of

$$\frac{|y|^2 \left| x - \frac{Ry}{|y|^2} \right|^2}{R^2} = |x - y|^2$$

for all $x \in \Gamma$ and $y \in \Omega$. Therefore, in view of Theorem 2.1, the inverse problem is equivalent to solving the system of integral equations

$$\varphi_p - \mu K' \varphi_p - \mu K_c' \varphi_p = 2\mu \frac{\partial}{\partial \nu} \Lambda(\cdot, x_p, x_{p+1}) \tag{3.2}$$

and

$$2(S\varphi_p)(x_q) - 2(S\varphi_p)(x_{q+1}) = \widetilde{V}_{pq} \tag{3.3}$$

for $q = 1, \ldots, n$, $q \notin \{p-1, p, p+1\}$ and $p = 1, \ldots, n$, where we abbreviated

$$\widetilde{V}_{pq} := V_{pq} - \Lambda(x_q, x_p, x_{p+1}) + \Lambda(x_{q+1}, x_p, x_{p+1}).$$

For obvious reasons we denote (3.2) as the field equations and (3.3) as the data equations.

From the various options for an iterative solution of (3.2) and (3.3) following ideas suggested by Johansson and Sleeman [**4**] in inverse obstacle scattering we propose the following alternating iteration procedure. Given an approximation for the boundary ∂D for $p = 1, \ldots, n$ we can solve the well-posed integral equation of the second kind (3.2) for the densities φ_p. Then, keeping the densities φ_p fixed we linearize the equation (3.3) with respect to ∂D to update the boundary approximation. This slightly deviates from the approach in [**1, 2, 7**] to linearize both equations simultaneously for ∂D and φ_p and avoids the need to adjust regularization parameters both for the boundary and the densities.

Since the right hand side of (3.3) represents only a finite number, that is, $n(n-3)$ voltage measurements we need to restrict the parameterizations z to some finite dimensional subspace V_M of dimension M of smooth 2π periodic functions from $\mathbf{R}$ into $\mathbf{R}^2$. We redefine the operator from (2.23) as an operator $A : H_0^{-1/2}[0, 2\pi] \times V_M \to H_0^{-1/2}[0, 2\pi]$ as

(3.4)
$$(A(\psi, z))(t) := \int_0^{2\pi} \{L(t, \tau; z) + L_c(t, \tau; z)\}\, \psi(\tau)\, d\tau, \quad t \in [0, 2\pi],$$

where we indicate the dependence of the kernels (2.21) and (2.22) on the parameterization z of ∂D. We also write $\lambda(\cdot, x_+, x_-; z)$ for the right-hand side in (2.25). Further, we introduce the operator $B : H_0^{-1/2}[0, 2\pi] \times V_M \to L^2(\Gamma)$ by

$$(B(\psi, z))(x) := \frac{1}{\pi} \int_0^{2\pi} \ln \frac{1}{|x - z(\tau)|}\, |z'(\tau)|\, \psi(\tau)\, d\tau, \quad x \in \Gamma. \tag{3.5}$$

Then the parameterized versions of (3.2) and (3.3) assume the form

$$\psi_p - \mu A(\psi_p, z) = 2\mu\lambda(\cdot, x_p, x_{p+1}; z) \tag{3.6}$$

and

$$(B(\psi_p, z))(x_q) - (B(\psi_p, z))(x_{q+1}) = \widetilde{V}_{pq}. \tag{3.7}$$

From [**9**] we know that B is Fréchet differentiable with respect to z with the derivative

$$\begin{aligned}(d_z B(\psi,z)(\xi))(x) &= -\frac{1}{\pi}\int_0^{2\pi} \frac{\{z(\tau)-x\}\cdot\xi(\tau)}{|z(\tau)-x|^2}\,|z'(t)|\psi(\tau)\,d\tau \\ &\quad -\frac{1}{\pi}\int_0^{2\pi} \frac{z'(\tau)\cdot\xi'(\tau)}{|z'(\tau)|}\ln(|z(\tau)-x|)\,\psi(\tau)\,d\tau, \quad x\in\Gamma.\end{aligned}$$

Now our iterative scheme proposed for the solution of the inverse problem is as follows. Assume that the curve with parameterization z is an approximation ∂D.

1. For $p=1,\dots,n$ the well-posed boundary integral equation (3.6) is solved for densities $\psi_p=\varphi_p\circ z$.

2. Keeping the densities fixed (3.7) is linearized, that is, we find $\xi\in V_M$ as a solution to the linear equations

$$\begin{aligned}(d_z B(\psi_p,z)(\xi))(x_q) - (d_z B(\psi_p,z)(\xi))(x_{q+1}) \\ = \widetilde{V}_{pq} - (B(\psi;z))(x_q) - (B(\psi;z))(x_{q+1})\end{aligned} \tag{3.8}$$

for $q=1,\dots,n$, $q\notin\{p-1,p,p+1\}$ and $p=1,\dots,n$.

3. The curve z is updated by $z+\xi$.

This scheme is iterated until some stopping criterium is satisfied.

In terms of a basis $z_1,\dots,z_M$ of 2π periodic functions $z_m:\mathbf{R}\to\mathbf{R}^2$ for V_M we represent

$$\xi=\sum_{m=1}^{M} a_m z_m \tag{3.9}$$

with real coeffizients a_m. Then after approximating the integrals in B and $d_z B$ by the composite trapezoidal rule, the linear system (3.8) reduces to an $n(n-3)\times M$ linear system for the coefficients a_m. There are redundancies in the voltage data since for all p and q with $p-q\notin\{-1,0,1\}$ by reciprocity we have

$$V_{pq}-V_{qp}=\frac{I}{\pi\sigma_0}\ln\left|\frac{x_p-x_{q+1}}{x_q-x_{p+1}}\right|$$

(which is zero for equidistant electrodes). Hence the linear system is overdetermined only if $n(n-3) \geq 2M$. For our numerical examples we used for V_M the space of trigonometric polynomials of degree less than or equal to N (mapping $\mathbf{R}$ into $\mathbf{R}^2$), that is, a space of dimension $M = 4N + 2$.

Since the linearized equation (3.8) inherits ill-posedness from the original nonlinear inverse problem, regularization is required. For this we applied Tikhonov regularization with the regularization parameter α chosen by the concept of a quasi-solution [**6**]. To explain the idea we rewrite (3.8) in the form

$$dF(z)\xi = \mathcal{V} - F(z)$$

where $F : V_M \to \mathbf{R}^{n(n-3)}$ with Fréchet derivative dF and $\mathcal{V} \in \mathbf{R}^{n(n-3)}$. In the case of perturbed data $\mathcal{V}_\delta$ with $\|\mathcal{V}_\delta - \mathcal{V}\| \leq \delta$ and a noise level δ this is replaced by

$$dF(z)\xi = \mathcal{V}_\delta - F(z). \tag{3.10}$$

Assume that $||F(z) - \mathcal{V}_\delta|| > ||\delta||$ which is reasonable since it does not make sense to reduce the residual under the noise level. The regularization α should be appropriate if we can ensure an approximate solution ξ_α such that $\|F(z+\xi_\alpha) - \mathcal{V}_\delta\|$ is minimal under the restriction $\|F(z+\xi_\alpha) - \mathcal{V}_\delta\| \geq \delta$. For this we choose

$$\rho = \frac{\|F(z) - \mathcal{V}_\delta\| - \delta}{\|dF(z)\|}\ . \tag{3.11}$$

Then for each ξ with $\|\xi\| \leq \rho$ we have that

$$\|F(z) - \mathcal{V}_\delta\| - \|dF(z)\xi\| \geq \delta,$$

and consequently

$$\|F(z) - \mathcal{V}_\delta\|^2 - 2\|F(z) - \mathcal{V}_\delta\|\,\|dF(z)\xi\| + \|dF(z)\xi\|^2 \geq \delta^2.$$

From this, using the Cauchy-Schwarz inequality, we deduce that

$$\|F(z+\xi) - \mathcal{V}_\delta\|^2 \approx \|F(z) + dF(z)\xi - \mathcal{V}_\delta\|^2 \geq \delta^2.$$

Hence, it seems to be reasonable to choose the regularization parameter in the Tikhonov regularization

$$\alpha\xi_\alpha + [dF(z)]^* dF(z)\xi = [dF(z)]^*[\mathcal{V}_\delta - F(z)]$$

such that the solution ξ_α is the quasi-solution of (3.10) with constraint ρ.

We conclude this section by noting that after the modification (2.27) for Φ_c the inverse scheme for the case of the half space as background medium is exactly the same as for the disk.

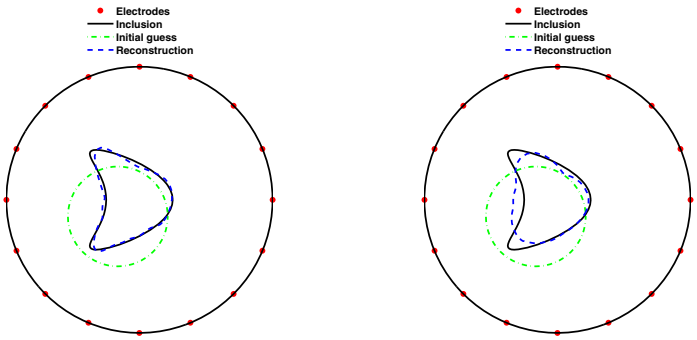

FIGURE 1. Reconstruction of kite-shaped domain (4.1) without noise (left) and 2% noise (right).

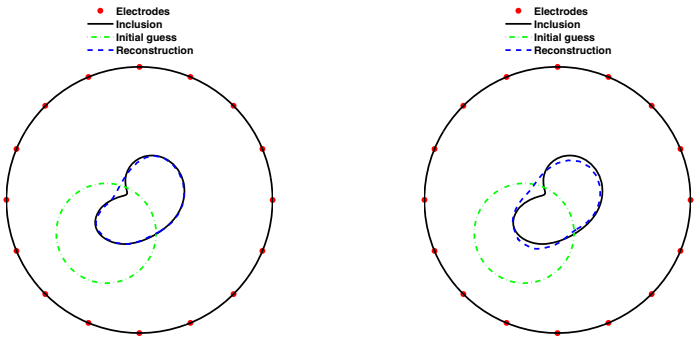

FIGURE 2. Reconstruction of bean-shaped domain (4.2) without noise (left) and 2% noise (right).

4. Numerical examples. We now present some numerical reconstructions based on synthetic data. For these the radius of the disk Ω is chosen $R = 4$, the values of the conductivities are $\sigma_0 = 1$ and $\sigma_1 = 2$. The number of the equidistantly spaced electrodes on Γ was chosen as $n = 16$. To start with we tested three configurations for the inclusion D, each of them without noise on the synthetic data and with 2% Gaussian noise. In the figures the exact boundaries are in full (black) lines and the reconstructions in dashed (blue) lines. The initial guess is indicated in dashed-dotted (green) lines.

The first example in Figure 1 is a kite-shaped domain with boundary parameterization

$$z(t) = (-0.65 + \cos t + 0.65\cos 2t, 1.5\sin t)\,, \quad t \in [0, 2\pi]. \tag{4.1}$$

The second example in Figure 2 is given by a bean-shaped domain with boundary

$$z(t) = 2.5\,\frac{0.5 + 0.4\cos t + 0.1\sin 2t}{1 + 0.7\cos t}\,(\cos t, \sin t)\,, \quad t \in [0, 2\pi]. \tag{4.2}$$

The third example in Figure 3 is a square with the corners $(1.5, 0)$, $(0, 1.5)$, $(-1.5, 0)$ and $(0, -1.5)$. For creating the synthetic data for the square the Nyström method was adjusted to cope with the corner singularities. In each case the degree of trigonometric polynomials was chosen as $N = 8$. For the kite-shaped domain, the initial guess is the circle of radius 1.5 centered at $(-0.65, -0.5)$. For the bean-shaped domain and for the square, the initial guess is the circle of radius 1.5 centered at $(-1, -1)$. Each reconstruction required less than ten seconds and though we ran thirty iterations in each example, the error level was reached between the twentieth and thirtieth iteration.

In order to test the inverse scheme for larger inclusions, in Figure 4 we present numerical results for a larger kite with parameterization

$$z(t) = 1.25\,(-0.65 + \cos t + 0.65\cos 2t, 1.5\sin t)\,, \quad t \in [0, 2\pi], \tag{4.3}$$

and a heart-lungs-shaped domain with parameterization

$$z(t) = 2(\cos t, 2\sin t)\sqrt{0.99^2\cos 2t + \sqrt{1 - 0.99^2\sin^2 2t}}, \quad t \in [0, 2\pi]. \tag{4.4}$$

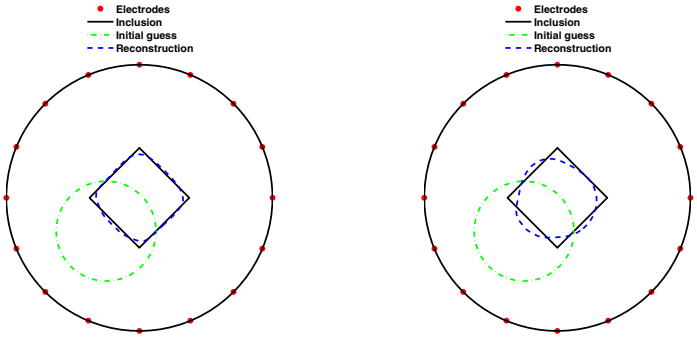

FIGURE 3. Reconstruction of square without noise (left) and 2% noise (right).

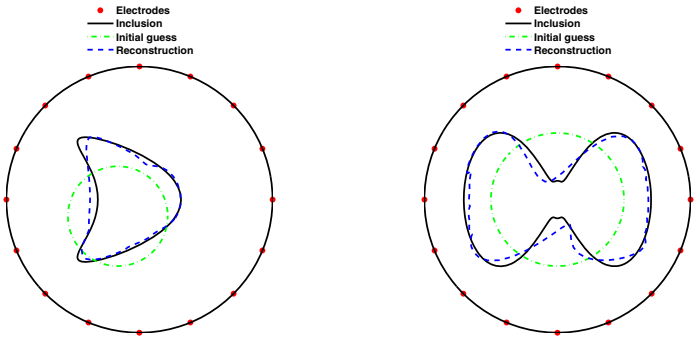

FIGURE 4. Reconstruction of kite-shaped domain (4.3) and heart-lungs-shaped domain (4.4) with 2% noise.

All other parameters are kept to be the same with the exception that the number of iterations for the heart-lungs-shaped domain has beenincreased to 50 with the initial guess a circle of radius 2 centered at the origin. Both reconstructions are with a 2% Gaussian noise on the synthetic data.

The next example illustrates that with appropriate modifications the method also can be applied to the reconstruction of more than one inclusion. Here the disk Ω has radius $R = 6$ and contains a kite-shaped and a bean-shaped inclusion. The background conductivity is $\sigma_0 = 1$

and the conductivities of the inclusions are $\sigma_{\text{kite}} = 2$ and $\sigma_{\text{bean}} = 3$. The parameterizations of the inclusions are given by

$$z_{\text{kite}}(t) = (-2.5, -1.5) + (-0.65 + \cos t + 0.65 \cos 2t, 1.5 \sin t) \tag{4.5}$$

and

$$z_{\text{bean}}(t) = (2.5, 1.5) + 2.5 \, \frac{0.5 + 0.4 \cos t + 0.1 \sin 2t}{1 + 0.7 \cos t} \, (\cos t, \sin t) \tag{4.6}$$

for $t \in [0, 2\pi]$. Deviating from the previous examples the approximation space V_M is chosen as cubic splines with 26 Bézier points for each of the two unknown boundary curves. The initial guess consists of two circles of radius 1 centered at $(-1, -3)$ for the kite and $(1, 3)$ for the bean. The result after 12 iterations is illustrated in Figure 5.

We conclude with examples for reconstructions with the background medium the lower half plane. Here, the 16 electrodes on Γ are spaced equidistantly in $[-8, 8] \times \{0\}$. Again in Figure 6 we consider a kite-shaped domain

$$z(t) = (-0.65 + \cos t + 0.65 \cos 2t, -3 + 1.5 \sin t), \quad t \in [0, 2\pi], \tag{4.7}$$

in Figure 7 a bean-shaped domain

$$z(t) = 3 \, \frac{0.5 + 0.4 \cos t + 0.1 \sin 2t}{1 + 0.7 \cos t} \, (\cos t, \sin t) - (0, 3), \; t \in [0, 2\pi] \tag{4.8}$$

and in Figure 8 a square $(1.5, -3)$, $(0, -1.5)$, $(-1.5, -3)$ and $(0, -4.5)$. The initial guess is the circle of radius 1.5 centered at $(-0.65, -4.5)$ for the kite-shaped domain, the circle of radius 2 centered at $(-0.65, -3.5)$ for he bean-shaped domain and the circle of radius 1.5 centered at $(-1, -1)$ for the square. All the other parameters are the same as in the case of the disk as background medium.

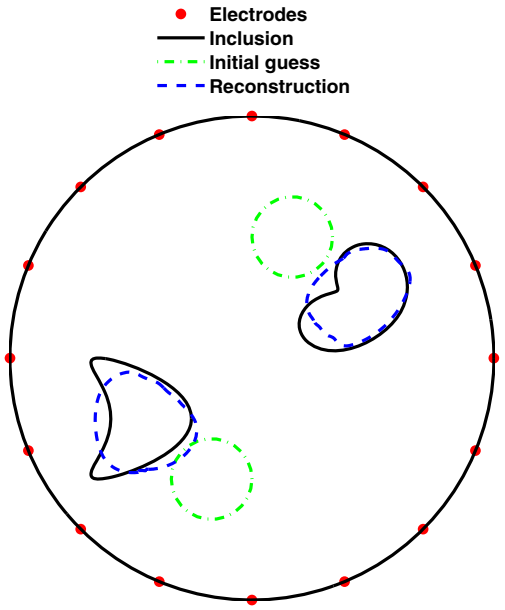

FIGURE 5. Reconstruction of two inclusions (4.5) and (4.6) with 1% noise.

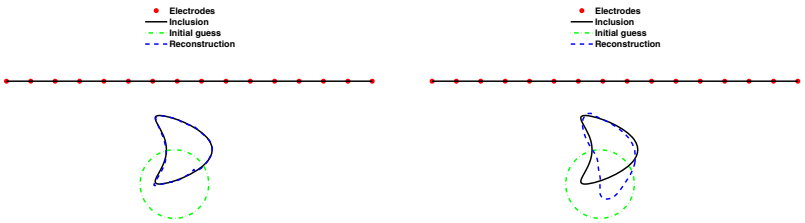

FIGURE 6. Reconstruction of kite-shaped domain (4.7) without noise (left) and 2% noise (right).

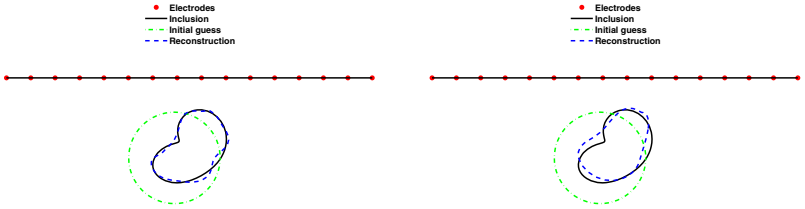

FIGURE 7. Reconstruction of bean-shaped domain (4.8) without noise (left) and 2% noise (right).

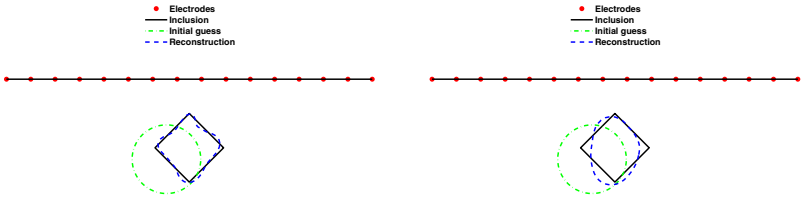

FIGURE 8. Reconstruction of square without noise (left) and 2% noise (right).

REFERENCES

1. H. Eckel and R. Kress, *Nonlinear integral equations for the inverse electrical impedance problem*, Inverse Problems **23** (2007), 475–491.

2. ———, *Nonlinear integral equations for the complete electrode model in inverse impedance tomography*, Appl. Anal. **87** (2008), 1267–1288.

3. M. Hanke and M. Brühl, *Recent progress in electrical impedance tomography*, Inverse Problems **19** (2003), S65–S90.

4. T. Johansson and B. Sleeman, *Reconstruction of an acoustically sound-soft obstacle from one incident field and the far field pattern*, IMA J. Appl. Math. **72** (2007), 96–112.

5. V. Kolehmainen, M. Lassas and P. Ola, *Inverse conductivity problem with an imperfectly known boundary*, SIAM J. Appl. Math. **21** (2005), 365–383.

6. R. Kress, *Linear integral equations*, 2nd ed. Springer-Verlag, Berlink, 1999.

7. R. Kress and W. Rundell, *Nonlinear integral equations and iterative solution for an inverse boundary value problem*, Inverse Problems **21** (2005), 1207–1223.

8. W. McLean, *Strongly elliptic systems and boundary integral equations*, Cambridge University Press, Cambridge, 2000.

9. R. Potthast, *Fréchet differentiability of boundary integral operators in inverse acoustic scattering*, Inverse Problems **10** (1994), 431–447.

10. E. Somersalo, M. Cheney and D. Isaacson, *Existence and uniqueness for electrode models for electric current computed tomography*, SIAM J. Appl. Math. **52** (1992), 1023–1040.

11. O. Steinbach and W.L. Wendland, *On C. Neumann's method for second-order elliptic systems in domains with non-smooth boundaries*, J. Math. Anal. Appl. **262** (2001), 733–748.

Institut für Numerische und Angewandte Mathematik, Universität Göttingen, 37083 Göttingen, Germany
Email address: delbary@math.uni-goettingen.de

Institut für Numerische und Angewandte Mathematik, Universität Göttingen, 37083 Göttingen, Germany
Email address: kress@math.uni-goettingen.de